Velocity of sound in relativistic heavy-ion collisions

Bedangadas Mohanty and Jan-e Alam
Variable Energy Cyclotron Centre, Calcutta 700 064, India
(Received 28 July 2003; published 11 December 2003)

We have studied the rapidity distribution of secondary hadrons produced in nucleus-nucleus collisions at ultrarelativistic energies within the ambit of the Landau's hydrodynamical model. A reasonable description of the data can also be obtained by using the Bjorken's hydrodynamical model if the boost invariance is restricted to a finite rapidity range. The sensitivity of the hadronic spectra on the equation of state vis-à-vis the velocity of sound has been discussed. The correlation between the velocity of sound and the freeze-out temperature has been indicated. The effects of the nonzero widths of various mesonic and baryonic degrees of freedom up to the mass value ~2.5 GeV are seen to be small.

DOI: 10.1103/PhysRevC.68.064903 PACS number(s): 25.75.Dw, 12.38.Mh

I. INTRODUCTION

One of the important problems in the field of relativistic heavy-ion collisions is to find out the equation of state (EOS) of the matter formed after nuclear collisions at ultrarelativistic energies [1]. Under the assumption of local thermal equilibrium, the EOS is the functional relation between pressure (P) and the energy density (ϵ), where P and ϵ are related through the velocity of sound c_s, which is defined as $c_s^2 = (\partial P/\partial \epsilon)_{isentropic}$ [2]. For a massless, noninteracting gas, $c_s^2 = 1/3$ (ideal gas limit). The velocity of sound plays a crucial role in the hydrodynamical evolution of the matter created in heavy-ion collision and affects, among others, the momentum distribution of the particles originating from the fluid elements at the freeze-out stage. In the present work we will assume the order of the phase transition from quark-gluon plasma (QGP) to hadrons to be first order. However, it should be mentioned here that this issue is not fully settled yet. The phase transition from QGP to hadrons could be weak first order, second order, or it may be just a crossover depending on the mass of the dynamical quarks [3]. Consider a situation where QGP is formed at the initial state. In such a scenario, the matter evolves from an initial QGP state to the hadronic phase via an intermediate mixed phase of QGP and hadrons due to the expansion of the system (hence cooling) in a first order phase transition scenario. Finally the system disassembles to hadrons (mainly pions) at the freeze-out where the interaction among the particles becomes too weak to maintain the equilibrium. The velocity of sound is very different in the three stages of expansion mentioned above, reflecting the interaction among the constituents of the matter in the three stages. While in the QGP phase, it should in principle approach the ideal gas limit, in the mixed phase it should reduce to zero due to vanishing pressure gradient, indicating "softness" of the EOS. Then below the critical temperature, it should have a value that reflects the presence of interacting hadrons in the system.

Relativistic hydrodynamical models have been routinely used to describe the multiplicity distribution in the rapidity space, transverse mass spectra of hadrons, etc., produced in nuclear collisions. One of the aims of the present work is to calculate the velocity of sound for hadronic system and compare the results with lattice QCD calculations. In the present calculation we have taken into account the nonzero width of the unstable hadrons. We study the rapidity distribution of the particles within the framework of relativistic hydrodynamical models proposed by Landau and collaborators [4] and by Bjorken [5]. The results of the analysis performed within these models will be compared with experiments to extract the velocity of sound. It is expected that at AGS and also at SPS energies, the Landau hydrodynamical model can be applied, although the Bjorken hydrodynamical model has been used at SPS energies. The main criticisms of Landau model are: (i) neglect of leading particle effects and (ii) removal of radiation energy due to the deceleration required in this model for full stopping. These difficulties, however, can be removed if one assume that during the collisions the valence quarks move without much interaction and the energy carried by the gluon fields is stopped in the collision volume [6]. This assumption is justified because the gluon-gluon interaction cross section is larger than quark-quark interaction due to larger color degeneracy of the gluons. The gluon field thermalizes after a time τ_i, providing the initial condition of the Landau model. In this picture the removal of energy of the decelerated gluons fields due to the bremsstrahlung is prohibited by the color confinement mechanism. Under these conditions, it is obvious that only a fraction of the beam energy is stopped in the collisions, which can be taken into account by introducing an inelasticity factor in the model [6].

Bjorken hydrodynamical model predicts a plateau structure for the rapidity distribution of the fluid elements which is not observed experimentally for the entire rapidity range. It has been indicated in Ref. [7] from perturbative QCD that the initial energy distribution is a broad Gaussian in rapidity even at LHC energies. However, we will show that a good description of the data is possible at AGS and SPS energies in the framework of Bjorken's model if we treat the upper limit of the fluid rapidity as a parameter. In other words, the boost invariance has to be limited in a finite rapidity range for the description of the data.

The paper is organized as follows. In the following section we obtain the velocity of sound for a hadronic model and compare the result with the lattice QCD calculations [3] and those obtained from a simple confinement model as dis-

TABLE I. Particles taken for calculation.

Baryons	Mesons
p	$\pi^{+,-,0}$
n	$\eta(547-1440)$, η'
$N(1440-2600)$	$f_0(800-1710)$, $f_1(1285, 1420)$, $f_2(1270-2340)$
$\Delta(1232-2420)$	$\rho(770-1700)$, ρ_3
$\Lambda(1115-2350)$	$\omega(782-1650)$, ω_3
$\Sigma^{+,-,0}$	$a_0(980-1450)$, a_1
$\Sigma(1382-1820)$	ϕ, ϕ_3, $\pi(1300-1800)$, π_2
$\Xi^{0,+}$	f_4, h_1, $K_1(1270-1400)$
$\Xi(1530-1820)$	a_2, a_4, b_1, K_2
Ω^-	$K^{\pm,0}$, $K^0_{L,S}$, K^*, $K^*_{0,2,3,4}$

cussed in Ref [8]. In Sec. III we extract the velocity of sound from the particle number density in rapidity space at AGS and SPS energies. Finally, in Sec. IV we present summary and discussions.

II. EQUATION OF STATE FOR HADRON GAS

For the study of the EOS for the hadronic gas we take all the hadrons as listed in the particle data book up to the strange sector. The complete list is given in Table I. The thermodynamical quantities such as energy density (ϵ) and pressure (P) can be calculated using the standard relations,

$$\epsilon = \sum_{hadrons} \frac{g}{(2\pi)^3} \int E(\vec{p}) f(E) \rho(M) dM^2 d^3p,$$

$$P = \sum_{hadrons} \frac{g}{(2\pi)^3} \int \frac{\vec{p}^2}{3E} f(\vec{p}) \rho(M) dM^2 d^3p, \qquad (1)$$

where $E=\sqrt{\vec{p}^2+M^2}$ is the energy of the particle of three-momentum $\vec{p}$ and invariant mass M, g represents internal degrees of freedom, and $f(E)$ is the well-known thermal distribution for bosons and fermions which is given by $f(\vec{p})=\{\exp[(E-\mu)/T]\pm 1\}^{-1}$, where μ is the chemical potential and T is the temperature. The summation in Eq. (1) is carried out for all the hadrons up to strange sector [9]. The sensitivity of the EOS on the hadronic and electromagnetic spectra has been studied in Ref. [10], with less number of hadrons and the widths of the hadrons are ignored. $\rho(M)$ denotes the spectral function of the hadrons of pole mass m and width Γ given by

$$\rho(M) = \frac{1}{\pi} \frac{M\Gamma(M)}{(M^2-m^2)^2 + M^2\Gamma^2}. \qquad (2)$$

Note that for stable particle $\rho(M) \to \delta(M^2-m^2)$ as $\Gamma \to 0$. To evaluate the spectral function of a hadron in a thermal bath one should consider all the elastic and inelastic processes through which the hadrons under consideration interact with all the constituents of the thermal bath [11]. These interactions give rise to the momentum dependent effective mass and widths. However, in the present work we restrict to the vacuum values of these quantities which are taken from Ref. [9]. The spectral function can also be related to the two body phase shift (δ) of the various processes as $\rho(M) \propto d\delta(M)/dM$, leading to the results obtained by S-matrix formalism of the statistical mechanics proposed by Dashen *et al.* [12].

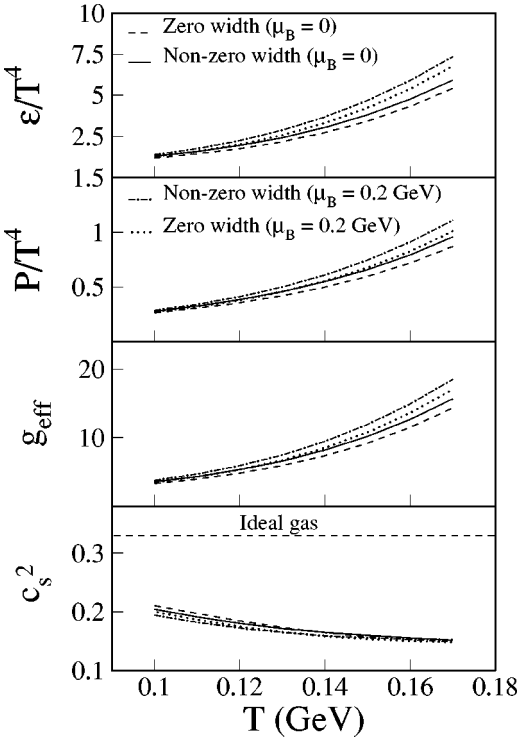

FIG. 1. Variation of energy density (ϵ), pressure (P), effective statistical degeneracy (g_{eff}), and velocity of sound (c_s) with temperature (T).

From Eq. (1) one can calculate the entropy density (s) by using the relation $s=(\epsilon+P-\mu n)/T$ where n is the net baryon density given by

$$n = \sum_{baryons} \frac{g}{(2\pi)^3} \int f(E) \rho(M) dM^2 d^3p,$$

g_{eff} is the effective degeneracy which is parametrized as $g_{eff}(\mu, T)=90s/(4\pi^2T^3)$. The velocity of sound for $\mu=0$ can be calculated from the g_{eff} as

$$c_s^{-2} = \frac{T}{s}\frac{ds}{dT} = 3 + \frac{T}{g_{eff}}\frac{dg_{eff}}{dT}. \qquad (3)$$

We will assume the chemical potential to be zero for mesons and consider two cases for baryonic chemical potential, $\mu=0$ and 200 MeV.

In Fig. 1 we plot the variation of various thermodynamic quantities: ϵ, P, g_{eff}, and c_s^2 as a function of temperature. We make two observations: (a) the effects of the finite width in the masses of the hadrons on the thermodynamical quantities turn out to be small and (b) the effect of the finite baryonic chemical potential leads to slightly larger values of ϵ, P, and g_{eff} but lower values of c_s^2 at a (typical) freeze-out temperature of 120 MeV.

For comparison of our results with those from the lattice QCD calculations [3], we parametrize the variation of energy density (ϵ) of lattice QCD results with temperature as follows [13]:

$$\epsilon = T^4 A \ \tanh\left[B\left(\frac{T}{T_c}\right)^C\right], \tag{4}$$

where A, B, and C are parameters whose values are 12.44, 0.517, and 10.04, respectively. Note that the effect of baryons in the EOS is neglected here.

The evolution of the system under the assumption of boost invariance along the longitudinal direction is governed by the equation [5]

$$\frac{d\epsilon}{d\tau} + \frac{\epsilon + P}{\tau} = 0, \quad P = c_s^2 \epsilon, \tag{5}$$

where c_s is the velocity of sound in the medium. We would like to mention here that the velocity of sound sets the expansion time scale $[(\tau_{exp})^{-1} \sim (1/\epsilon) d\epsilon/d\tau = (1+c_s^2)/\tau]$ for the system. This time scale should be larger than the collision time scale $[(\tau_{coll})^{-1} \sim n\sigma v$, where σ is the cross section, v is velocity, and n is density] for thermal equilibrium to be maintained in the system. Therefore, determination of velocity of sound becomes very important for the study of the space time evolution of the system in general and hadronic spectra in particular.

We obtain the expression for the velocity of sound as (see also Ref. [13])

$$c_s^2 = \left[3 + BC\left(\frac{T}{T_c}\right)^C \frac{1}{\cosh[B(T/T_c)^C] \sinh[B(T/T_c)^C]}\right]^{-1}. \tag{6}$$

The results for the confinement model were obtained from Ref. [8] by extracting $g_{eff}(T)$ by using the relation $\epsilon/T^4 = (\pi^2/30) g_{eff}$ and Eq. (3).

In Fig. 2 the energy density, effective statistical degeneracy, and the velocity of sound evaluated in the hadronic model at zero baryonic chemical potential are compared with the lattice data (μ=0) and those obtained form the confinement model. We observe the following.

(a) Our results match with those from the lattice and the confinement model near T_c.

(b) They are higher than those obtained from lattice below T_c. (In this context we would like to point out two things. First, lattice results usually employ quark masses which are too large, leading to larger pion masses, $m_\pi^{lat} \geqslant 3 m_\pi^{physical}$. The resulting thermal suppression of these degrees of freedom causes a considerable discrepancy for lattice EOS with respect to EOS for hadron gas. Second, the lattice calculations below T_c have large errors.)

(c) At temperatures below T_c the velocity of sound shows an interesting trend, it increases with decrease in temperature, then falls to zero as temperature of the system approaches zero.

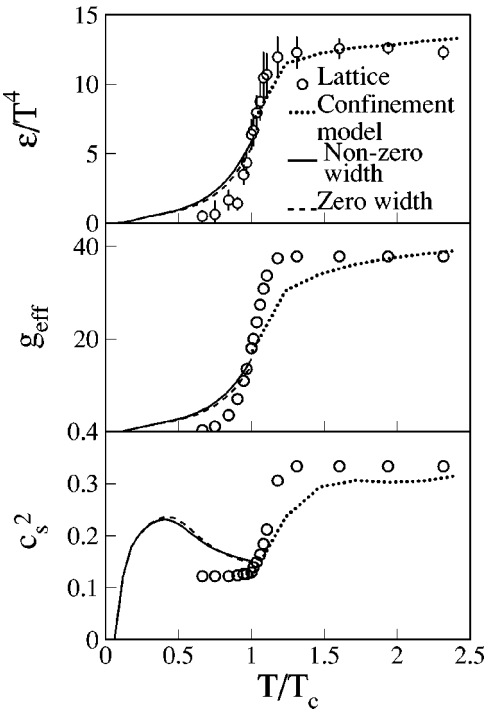

FIG. 2. Variation of energy density, g_{eff}, and velocity of sound using the combined results of hadron gas, confinement model, and lattice calculations with temperature. The lattice results for energy density have been read from Ref. [3]. g_{eff} and c_s^2 are derived by using the equations mentioned in the text.

(d) The complete EOS for the system with initial QGP state, may be those obtained from lattice for temperatures above T_c and those given by the present calculations for temperatures below T_c.

The velocity of sound, which is an input to the hydrodynamical evolution of the system via EOS, influences the rapidity distribution of the hadrons. In the following section we try to extract the velocity of sound from the rapidity distributions of various hadrons produced from heavy-ion collisions for various collision energies using hydrodynamical model. We then compare the values obtained with the results of the model under consideration.

III. RAPIDITY DISTRIBUTION OF SECONDARIES AT AGS AND SPS ENERGIES

There are two well known hydrodynamical models, as mentioned before [4,5], for the description of the space time evolution of the system formed after the collision of heavy ions. It may be mentioned that in the coherent interactions the collective effect is an important feature, unlike incoherent collisions where collision is considered to be a succession of independent nucleon-nucleon interactions. The basic difference is, in Landau's model, in the center of mass of the collision two nuclei would be stopped and all the kinetic energy would be used up for the particle production, while the baryon transparency in the midrapidity region is the basic feature of Bjorken's model. However, Landau's model can be applied to describe the system formed after nuclear colli-

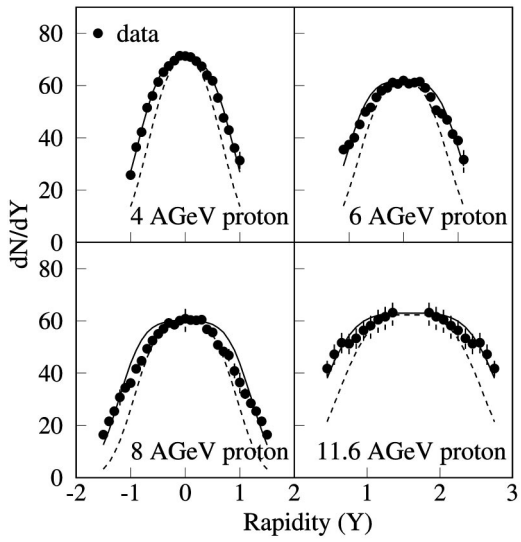

FIG. 3. Rapidity spectra for protons at 4*A*, 6*A*, 8*A*, and 11.6*A* GeV Au+Au collisions compared to rapidity spectra obtained from Landau hydrodynamics with velocity of sound 0.2 (solid line) and 0.333 (dashed line).

sion with appropriate initial conditions as mentioned in the Introduction. It is expected that the Landau hydrodynamics will work well at AGS and may be at SPS energies, while the Brojken hydrodynamics should, in principle, work well for energies at RHIC and LHC.

In the following we briefly discuss the rapidity distribution of the particles produced in relativistic heavy-ion collisions in Landau and Brojken models.

The amount of entropy (dS) contained within a (fluid) rapidity dy in the Landau hydrodynamical model is given by [4,14],

$$\frac{dS}{dy} = -\pi R^2 l s_0 \beta c_s \exp[\beta\omega_f]\left[I_0(q) - \frac{\beta\omega_f}{q} I_1(q)\right], \quad (7)$$

where $q=\sqrt{\omega_f^2 - c_s^2 y^2}$, $\omega_f = ln(T_f/T_0)$, T_f is the freeze-out temperature, y is the rapidity, R is the radius of the nuclei, $2l$ is the initial length, s_0 is the initial entropy density, $2\beta=(1-c_s^2)/c_s^2$, and I_0,I_1 are the Bessel's functions. The quantity $\pi R^2 l s_0$ is fixed to normalize the experimental data at the midrapidity. For $\omega_f \gg c_s y$ the quantity dS/dy can be approximated by a Gaussian distribution,

$$\frac{dS}{dy} \sim \text{const} \frac{\exp\left(-\frac{y^2}{2\sigma^2}\right)}{\sqrt{2\pi\sigma^2}}, \quad (8)$$

where $\sigma = 2\omega_f/(1-c_s^2)$.

The entropy density in the Brojken hydrodynamics is given by [14]

$$\frac{dS}{dy} = \frac{A\pi R^2}{T_f} s_f \exp[-2\beta\omega_f], \quad (9)$$

where A is a constant and s_f is the entropy density at the freeze-out. It is to be noted that the quantity dS/dy is independent of the rapidity in accordance with the assumption of boost invariance along the longitudinal direction [5].

TABLE II. AGS results.

Type (GeV)	c_s^2	χ^2	Probability
Proton 4*A*	1/5 (1/3)	0.65 (34.5)	1.0 (0.023)
Proton 6*A*	1/5 (1/3)	2.15 (40.2)	1.0 (0.010)
Proton 8*A*	1/5 (1/3)	7.1 (74.8)	0.999 (0.00001)
Proton 11.6*A*	1/5 (1/3)	1.49 (31.1)	1.0 (0.0388)

The multiplicity distribution of the secondaries is obtained by folding the multiplicity density in rapidity space mentioned above by the thermal distribution of the fluid elements,

$$\frac{dN}{dY} = \frac{g}{(2\pi)^3} \int \frac{dN}{dy} f(M_T, y, Y) M_T \cosh(Y-y) dy d^2 p_T, \quad (10)$$

where dN is the number of particles within the rapidity interval dY, M_T is the transverse mass ($=\sqrt{p_T^2+M^2}$) of the particle, $E=M_T\cosh(Y-y)$ is the energy and $f(E) = (1/\exp[E/T]\pm 1)$. dS/dy is related to dN/dy by a constant factor (see Ref. [13] for details). Performing the p_T integration in the above equation, we obtain

$$\frac{dN}{dY} \propto T^3 \int \frac{dN}{dy} h(y, Y; m, T) \exp[-m\cosh(Y-y)/T]\, dy, \quad (11)$$

where

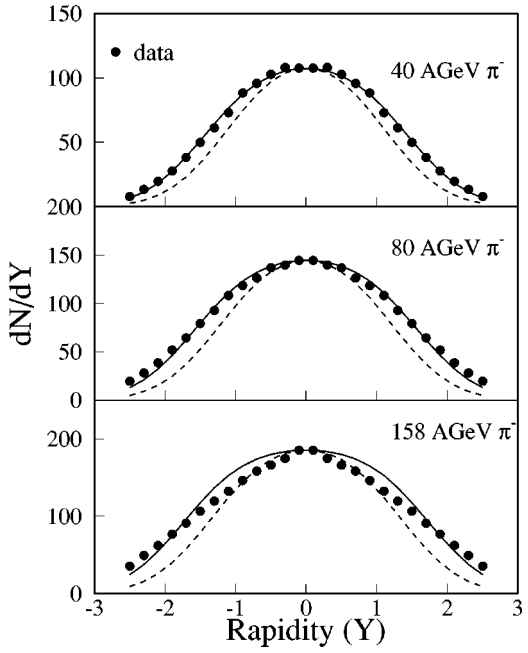

FIG. 4. Rapidity spectra for pions at 40*A*, 80*A*, and 158*A* GeV Pb+Pb collisions compared to rapidity spectra obtained from Landau hydrodynamics with velocity of sound 0.2 (solid line) and 0.333 (dashed line).

TABLE III. SPS results for pions.

Type (GeV)	c_s^2	χ^2	Probability
π^- 40*A*	1/5 (1/3)	1.03 (51.7)	1.0 (0.0013)
π^- 80*A*	1/5 (1/3)	2.6 (66.3)	0.999 (7×10^{-7})
π^- 158*A*	1/5 (1/3)	19.0 (146.0)	0.80 (4×10^{-19})

$$h(y, Y; m, T) = \frac{m^2}{T^2} + 2\frac{m}{T}\frac{1}{\cosh(Y-y)} + \frac{2}{\cosh^2(Y-y)}. \tag{12}$$

It may noted from Eqs. (11) and (12) that the particle mass tends to make the rapidity distribution narrower.

It may be mentioned that, while in Landau's model the width of the rapidity distribution is sensitive to the velocity of sound and the freeze-out temperature, in the case of Bjorken's model it is not (because of its independence of rapidity, the quantity, dS/dy can be fixed here by the normalization at the midrapidity). While integrating over y in Eq. (11), we treat the range of y as a parameter in case of Bjorken's hydrodynamics [15]. In case of Landau's hydrodynamics the integration limit for rapidity is infinite. We apply Landau's model to the rapidity distributions of the produced hadrons at AGS and SPS energies. It will be seen later that Landau model fits the pion rapidity spectra well at lower SPS energies, however at highest SPS energy the description is not very satisfactory, therefore we do not attempt to apply the model to RHIC energies. We fix the freeze-out temperature T_f to be 120 MeV a value obtained by studying the transverse momentum distributions of the hadrons [16,17].

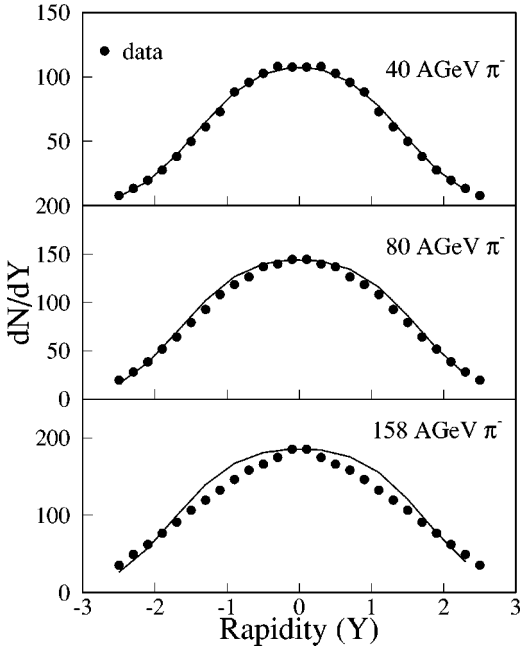

FIG. 5. Rapidity spectra for pions at 40*A*, 80*A*, and 158*A* GeV Pb+Pb collisions compared to rapidity spectra obtained from Bjorken's hydrodynamics. The values of $y_{max}(=-y_{min})$ used in the integration of Eq. (11) are 1.44, 1.65, and 1.6 for beam energies 40*A* GeV, 80*A* GeV, and 158*A* GeV, respectively.

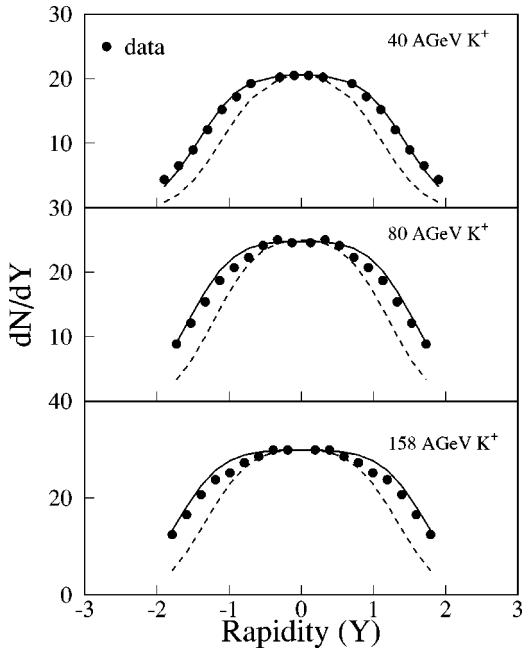

FIG. 6. Rapidity spectra for K^+ at 40*A*, 80*A*, and 158*A* GeV Pb+Pb collisions compared to rapidity spectra obtained from Landau hydrodynamics with velocity of sound 0.2 (solid line) and 0.333 (dashed line) and T_f=120 MeV.

The rapidity distributions of the protons [18,19] at AGS energies are well described by the Landau hydrodynamical model with velocity of sound, c_s^2=1/5, a value different from that corresponding to an ideal gas (Fig. 3). For c_s^2=1/5 the

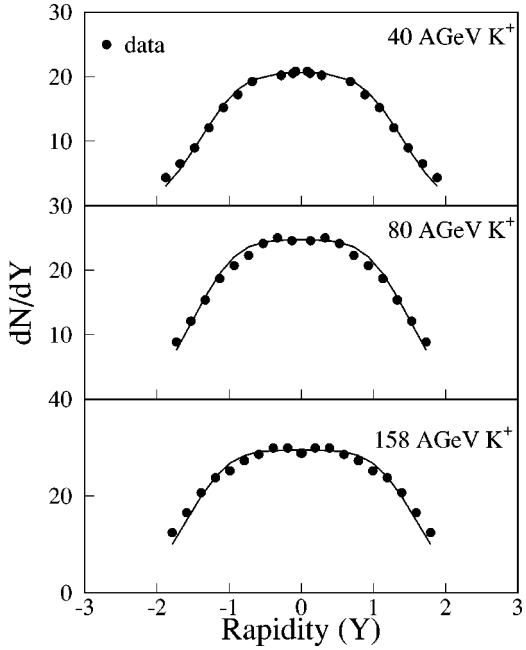

FIG. 7. Rapidity spectra for kaons at 40*A*, 80*A*, and 158*A* GeV Pb+Pb collisions compared to rapidity spectra obtained from Bjorken's hydrodynamics. The values of $y_{max}(=-y_{min})$ used in the integration of Eq. (11) are 1.4, 1.5, and 1.6 for beam energies 40*A* GeV, 80*A* GeV, and 158*A* GeV, respectively.

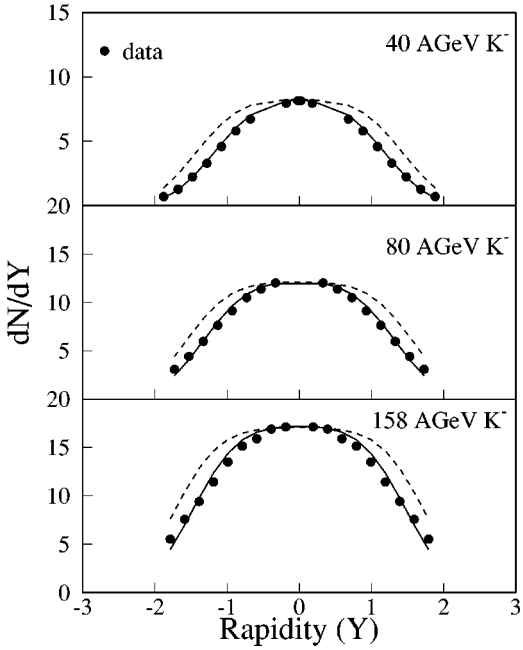

FIG. 8. Rapidity spectra for K^- at 40*A*, 80*A*, and 158*A* GeV Pb+Pb collisions compared to rapidity spectra obtained from Landau hydrodynamics with velocity of sound 0.2 for T_f =120 MeV (dashed line) and 132 MeV (solid line).

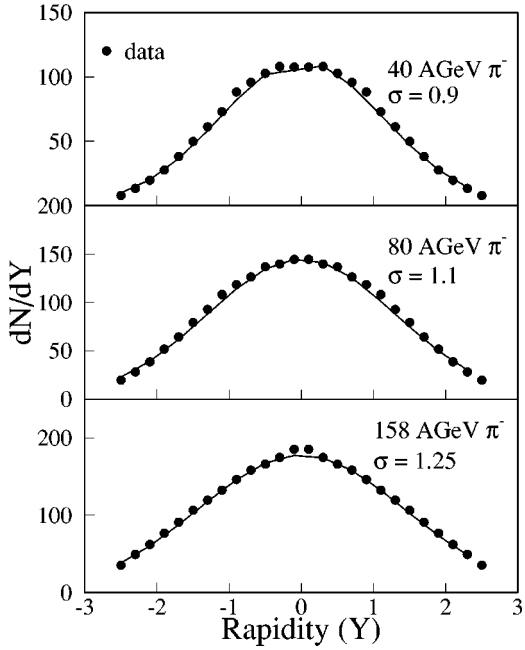

FIG. 9. Rapidity spectra for pions at 40*A*, 80*A*, and 158*A* GeV Pb+Pb collisions compared to rapidity spectra obtained from Eqs. (8) and (11). The width of the Gaussian in Eq. (8) is a parameter here.

value of the chi square is considerably smaller than for c_s^2 =1/3 (Table II). The peak of the distribution at the midrapidity in the experimental data seems to indicate a large deposition of collision energy in these interactions, where the Landau's hydrodynamical picture is applicable.

For SPS energies the density of pions in rapidity space [20] is well reproduced (Fig. 4) within the ambit of Landau's model with c_s^2=1/5 and T_f=120 MeV for 40 and 80 GeV/nucleon beam energies. For E_{beam}=158 GeV/nucleon the χ^2 worsens (Table III). The Bjorken's model also does not give a satisfactory description of the data at higher SPS energies (158*A* GeV). However, as shown in Fig. 5 at lower energies, Bjorken's model gives a reasonable description of the data.

Interestingly, the K^+ spectra are well reproduced (Figs. 6 and 7) with the same freeze-out temperature and velocity of sound as mentioned above for all the beam energies for both the models. However, the K^- spectra (Fig. 8) are reproduced with a slightly higher freeze-out temperature, 132 MeV. A good description of the data for 40 and 80 GeV/nucleon beam energies is also obtained for T_f =120 MeV and c_s^2=1/3.5 (χ^2=0.1 and 0.3, respectively). For E_{beam}=158 GeV/nucleon we obtain c_s^2=1/4 for same freeze-out temperature (χ^2=0.3). The values of χ^2 are shown in Table IV. It is well known that the system formed in nuclear collisions at AGS and SPS energies has nonzero baryonic density and in such a situation the differences in the values of the freeze-out parameters for K^+ and K^- are expected (see Ref. [21] for details).

The pion data from SPS at 40*A*, 80*A*, and 158*A* GeV energies can also be reproduced if we use the Gaussian ap-

TABLE IV. SPS results for kaons.

Type (GeV)	c_s^2	χ^2	Probability
K^+ 40*A*	1/5 (1/3)	0.463 (18.0)	1.0 (0.38)
K^- 40*A*	1/5 (1/3.3)	0.56 (0.16)	1.0 (1.0)
K^+ 80*A*	1/4.5 (1/3)	0.4 (12.7)	1.0 (0.75)
K^- 80*A*	1/5 (1/3.3)	3.0 (0.67)	0.99 (1.0)
K^+ 158*A*	1/4.5 (1/3)	0.39 (15.6)	1.0 (0.55)
K^- 158*A*	1/5 (1/3.5)	3.8 (0.8)	0.99 (1.0)

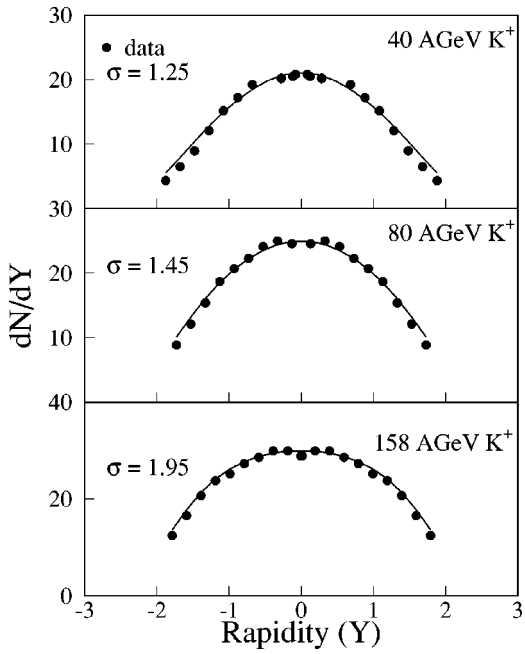

FIG. 10. Same as Fig. 9, but for kaons.

proximation of Eq. (8) in Eq. (11) and treat the width of the Gaussian (σ) as a parameter. Results are shown in Fig. 9. The value of σ=0.9, 1.1, and 1.25 for pion at beam energies 40*A*, 80*A*, and 158*A* GeV, respectively. Results obtained for kaons in this procedure are shown in Fig. 10. It is important to note that the values of the widths of the Gaussian which represent the rapidity distribution of the fluid elements are 1.25, 1.45, and 1.95 for 40*A*, 80*A*, and 158*A* GeV energies, respectively, and these values of σ are consistently higher than the values obtained for pions. The difference can be attributed to the mass difference between pions and kaons because pions and kaons are subjected to the same longitudinal flow velocity.

In Fig. 11 we show the constant χ^2 contour in the c_s^2-T_f plane. The results indicate that we need a value of c_s^2 less than 1/3 for a reasonable description of the data. We observe that $c_s^2 \sim 1/5$ near the freeze-out for different collision energies and for various hadronic species. This indicates a certain kind universality for the hadronic matter produced in heavy-ion collisions at a late stage of the evolution (freeze-out).

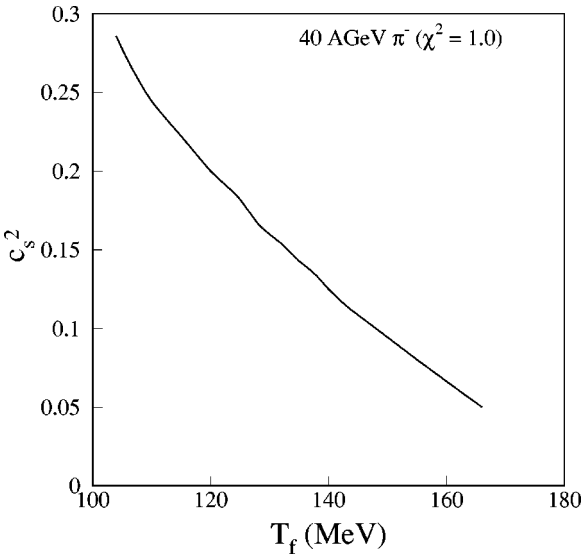

FIG. 11. The constant χ^2 contour in c_s^2-T_f plane for pions.

IV. SUMMARY

We have evaluated the velocity of sound in a hadronic model with hadronic degrees of freedom up to the strange sector. This calculated velocity of sound is compared with the results obtained from lattice QCD calculations [3] and those obtained for the confinement model [8]. The values compare well at the critical temperature. The effect of nonzero width of hadrons on the EOS is found to be small. Taking a nonzero baryonic chemical potential slightly decreases the velocity of sound. Fixing the value of the freeze-out temperature ($\sim$120 MeV) from the p_T spectra of hadrons [16,17] we find that a value of c_s^2=1/5 give a good description of the data for Landau's hydrodynamical model. The data are also well reproduced within the ambit of the hydrodynamical model proposed by Bjorken if the boost invariance is restricted to finite rapidity range. The value of c_s^2 =1/5 indicates that the expansion of the system is slower in comparison to the ideal gas scenario (c_s^2=1/3) and hence for such a system the maintenance of thermal equilibrium becomes easier. We observe that different hadron species produced in the nuclear collisions at different energies are well reproduced by a value of $c_s^2 \sim 1/5$, indicating some kind of universality of the matter at the freeze-out stage.

Several other effects which are ignored in the present work need to be mentioned at this juncture. For a complete description of the space time evolution of the system formed after heavy ion collisions both the transverse and longitudinal expansions should be considered. The transverse momentum spectra of the hadrons are strongly affected by the transverse flow. The rapidity distribution of the hadrons which is obtained after integrating out the transverse momentum may not be strongly affected by the transverse flow. However, the normalization of the rapidity spectra may be substantially affected by the transverse flow. The other quantities which may affect the normalization include nonzero chemical potential of the mesons, arising from the lack of chemical equilibrium in the system. The hadrons (pions, kaons, and protons) originating for the decays of various mesonic (ρ, ω, ϕ, etc.) and baryonic (Δ, etc.) resonances are ignored here. If the distribution of the resonances is homogeneous in the rapidity then the effects of the hadrons originating from their decays on the rapidity distributions can be ignored, otherwise these effects may change the distribution depending on the degree inhomogeneity and the abundances of the resonances at the freeze-out point. With the centrality of the collisions the normalization and the width of the distribution of hadrons in rapidity space changes. The normalization in the present work is treated as a parameter and the change in the width with centrality is rather small. At 158*A* GeV SPS energy the width of the rapidity distribution of a charged particle increases from 1.5 to 1.62 when the centrality changes from (0–5)% to (25–35)% [22].

ACKNOWLEDGMENTS

One of us (B.M.) is grateful to the Board of Research on Nuclear Science and Department of Atomic Energy, Government of India for financial support. We would also like to thank Marco van Leeuwen of NA49 Collaboration and Jennifer L. Klay of E895 Collaboration for providing the experimental data.

[1] *Proceedings of Quark Matter '2001*, edited by T. J. Hallman, D. E. Kharzeev, J. T. Mitchell, and T. Ullrich [Nucl. Phys. **A698**, 1 (2002)].
[2] L. D. Landau and E. M. Lifshitz, *Fluid Mechanics* (Pergamon, Oxford, 1975).
[3] F. Karsch, Nucl. Phys. **A698**, 199 (2002).
[4] L. D. Landau, Izv. Akad. Nauk. SSSR **17**, 51 (1953); S. Belenkij and L. D. Landau, Usp. Fiz. Nauk **56**, 309 (1955); Nuovo Cimento, Suppl. **3**, 15 (1956); *Collected Papers of L. D. Landau*, edited by D. ter Haar (Gordon and Breach, New York, 1965) p. 665.
[5] J. D. Bjorken, Phys. Rev. D **27**, 140 (1983).
[6] P. Caurruthers and M. Duong-Van, Phys. Rev. D **28**, 130 (1983); S. Pkokorski and L. Van Hove, Acta Phys. Pol. B **5**, 229 (1974); L. Van Hove and S. Pokoroski, Nucl. Phys. **B86**, 243 (1975).
[7] K. J. Eskola, K. Kajantie, and P. V. Ruuskanen, Eur. Phys. J. C **1**, 627 (1998).
[8] R. A. Schneider and W. Weise, Phys. Rev. C **64**, 055201 (2001).
[9] R. M. Barnett *et al.*, Particle Data Group, Phys. Rev. D **54**, 1 (1996).
[10] J. Sollfrank, P. Huovinen, M. Kataja, P. V. Ruskanen, M. Prakash, and R. Venugopalan, Phys. Rev. C **55**, 392 (1997).
[11] H. A. Weldon, Ann. Phys. (N.Y.) **228**, 43 (1993).
[12] R. Dashen, S. K. Ma, and H. J. Bernstein, Phys. Rev. **187**, 345 (1969).
[13] B. Mohanty, J. Alam, and T. K. Nayak, Phys. Rev. C **67**, 024904 (2003).
[14] D. K. Srivastava, J. Alam, S. Chakrabarty, S. Raha, and B. Sinha, Ann. Phys. (N.Y.) **228**, 104 (1993); Phys. Lett. B **278**, 225 (1992).
[15] E. Schnedermann, J. Solfrank, and U. Heinz, Phys. Rev. C **48**, 2462 (1993).
[16] B. K. Patra, J. Alam, P. Roy, S. Sarkar, and B. Sinha, Nucl. Phys. **A709**, 440 (2001).
[17] H. Appelshaser *et al.*, Phys. Rev. Lett. **82**, 2471 (1999).
[18] J. L. Klay *et al.*, E895 Collaboration, nucl-ex/0111006.
[19] L. Ahle *et al.*, Phys. Rev. C **60**, 064901 (1999).
[20] M. van Leeuwen *et al.*, NA49 Collaboration, Nucl. Phys. **A715**, 161 (2003).
[21] U. Heinz, K. S. Lee, and E. Schnedermann, in *Quark Gluon Plasma*, edited by R. C. Hwa (World Scientific, Singapore, 1990).
[22] M. C. Abreu *et al.*, NA50 Collaboration, Phys. Lett. B **530**, 43 (2002).